5

Sensors for Quality Control in Welding

Sadek C. Absi Alfaro
The Brasilia University, UnB
Brasil

1. Introduction

The welding process is used by many manufacture companies and due to this wide application many studies have been carried out in order to improve the quality and to reduce the cost of welded components. Part of the overheads is employed in final inspection, which begins with visual inspection, followed by destructive and non-destructive testing techniques. In addition to cost raise, final inspection is conducted when the part is finished only. When a defect occurs during welding, it can be reflected in the physical phenomena involved: magnetic field, electric field, temperature, sound pressure, radiation emission and others. Thus, if a sensor monitor one of these phenomena, it is possible to build a system to monitor the weld quality.
For the automation and control of complex manufacturing systems, a great deal of progress came up in the last decade, with respect to precision and on-line documentation (bases for the quality control). With the advent of electrically driven mechanical manipulators and later the whole, relatively new, multidisciplinary mechatronic engineering, the need of information acquisition has increased. The acquisition is, in many cases, distributed through the system, with strong interaction between the robot and its environment. The design objective is to attain a flexible and lean production. The requirement of real time processing of data from multisensor systems with robustness, in industrial environment, shows the need for new concepts on system integration.
A Multisensor system represents neither the utilization of many sensors with the same physical nature nor many independent measurement systems, but mainly sensor fusion, the extraction of global information coming from the interrelation data given by each sensor. Some examples are the estimation of the slope of any surface using two or three individual sensors, the simultaneous acquisition of the parameters of the automatic welding process MIG/MAG ("Metal Inert Gas/ Metal Active Gas") or the direct observation of the welding pool related to the control of current, voltage, wire speed and torch welding speed.
Technology advancements seek to meet the demands for quality and performance through product improvements and cost reductions. An important area of research is the optimization of applications related to welding and the resultant cost reduction. The use of non-destructive tests and defect repair are slow processes. To avoid this, online monitoring and control of the welding process can favor the correction and reduction of many defects before the solidification of the melted/fused metal, reducing the production time and cost.
With continuing advancements in digital and sensor technology, new methods with relatively high accuracy and quick response time for identification of perturbations during the welding process have become possible. Arc position, part placement variations, surface

contaminations and joint penetration are key variables that must be controlled to insure satisfactory weld production (Chen et al., 1990).
The techniques related to welding process optimization are based on experimental methodologies. These techniques are strongly related to experimental tests and seek to establish relations between the welding parameters and welding bead geometry. The introduction of close or adaptive control to welding processes must be done by monitoring a variable or set of variables which can identify a process disturbance. For each practical implementation of an adaptive system to a welding process one should identify the "envelope" or the set of monitoring variables. These variables must be used as a reference value in the process control, making the system control start with a parameter adjustment (welding current, voltage, etc.) to guarantee bead characteristics close to desirable values. The welding parameters vary in accordance to base material, type of chosen process, plate dimensions and welding bead geometry, so the adjustment of the reference value of a monitored variable will depend on the establishment of a set of optimized parameters which provide a welding bead with desirable specifications.
Researches related to adaptive systems for welding seek the improvement of welding bead geometry with direct (if based on monitoring sensors) or indirect monitoring techniques. The indirect monitoring systems are the more used, looking to link elements such as welding pool vibrations, superficial temperature distribution and acoustic emissions to size, geometry or welding pool depth (Kerr et al., 1999). The most used approaches in welding control are infrared monitoring, acoustic monitoring, welding pool vibrations and welding pool depression monitoring (Luo et al., 2000).
Aiming to optimize human analysis during the defect identification process, many researches were conducted to develop alternative techniques for automatic identification of defects considering different classes of signals such as plasma spectrum (Mirapeix et al., 2006), ultrasonic (Fortunko, 1980), computer vision (Liu et al. 1988), etc.
Three levels of "on-line" quality control have been adopted by the industry (see Fig. 1). In the first level, it should be able to automatically detect "on-line" bad welding joint production. In the second level, it should be able to search and to identify the fault and which are the reasons for the fault occurrence (changes in welding process induced by disturbances in shielding gas delivery, changes in wire feed rate and welding geometry, etc). In the third level, it should be able to correct welding parameters during the welding process to assure proper weld quality (Grad et al., 2004). The conventional parameters are usually used to detect and to identify defects. Moreover, the non-conventional parameters, at the present, are not used enough to evaluate the welding quality. They are some non-contact methods for welding monitoring process as acoustical sensing (Drouet, 1982; Mansoor, 1999; Yaowen, 2000; Tam, 2005; Poopat, 2006; Cayo, 2007, 2008, 2009), spectroscopy emission (Lacroix, 1999; Alfaro, 2006; Mirapeix, 2007), infrared emission (Nagarajan, 1992; Wikle, 1999; Fan, 2003) and sensoring combination (Alfaro et al. 2006).

2. Case studies

2.1 Spectroscopy

The science responsible for the study of the radiation emission is called spectroscopy. The physical phenomena consist on a photon emission in a determined wavelength or frequency after the absorption of some energy. Atoms, ions and molecules can emit photons in different wavelengths, but a wavelength is related only to one atom or ion or molecule. This

can be compared to a fingerprint. Thus, with this property it is possible to know what chemical element, ion or molecule is found at the reading area.
It is possible to improve a non-destructive and on-line weld defects monitoring system through the radiation emitted by the plasma present in the electric arc. Some spectral lines involved in the welding process are chosen and their intensity is measured by a spectrometer sensor. One objective is to evaluate whether the spectrometer is capable of sensing disturbances in the electric arc. Another goal is to determine change detection techniques able to point those disturbances.

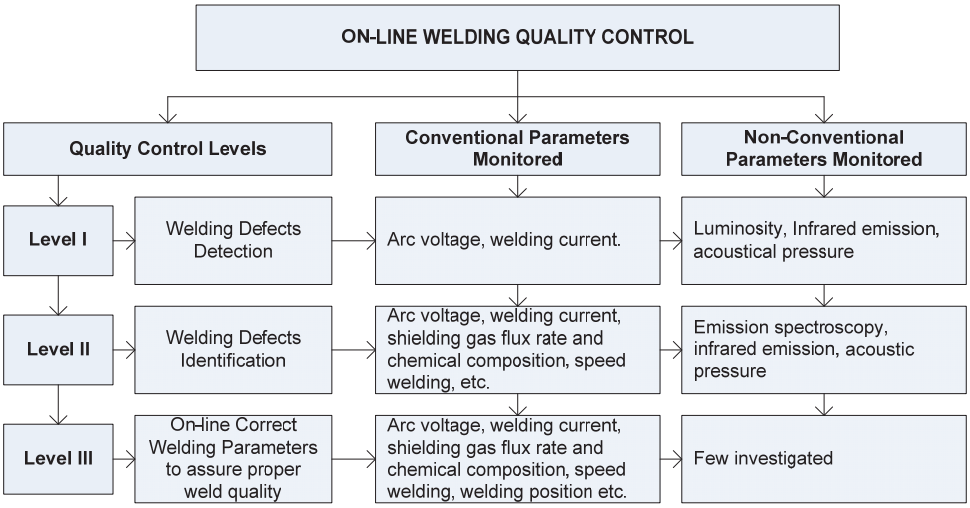

Fig. 1. On-line Welding Quality Control Levels.

Two analyses can be made with this information: qualitative and quantitative. In a qualitative approach, one is concerned in what elements are found on the plasma. And as a quantitative study, the objective is to evaluate some information extracted by the spectral taken. Therefore, a spectrometer could be applied as a sensor in a manufacturing process, such as welding, to detect the presence of some chosen elements or substances, like Iron, Cooper, water, grease; or to monitor significant changes of the energy emitted by some elements.
For example, in a stable GTAW the spectrum of the electric arc is stable as well. The amount of shielding gas, vaporized and melted steel, and other elements found at the electric arc are quite constant; therefore, if reflects on a stable spectrum. If a quantity of any element changes it will reflect on higher or lower emission energy. If different elements are introduced on the process, it will raise the energy of those elements.
An ordinary factor applied as a quantitative evaluation is the calculation of the plasma Electronic Temperature. Another that can be applied is the intensity of radiation emitted by some spectral lines. The Electronic Temperature can be calculated with different techniques, one is the relative intensity of spectral lines, of the transition from the level m to r of one line and from j to i of the other line, given by Equation 1 (Marotta, 1994)

$$T_e = \frac{E_m - E_j}{K_B \cdot \ln\left(\frac{E_m \cdot I_{ji} \cdot A_{mr} \cdot g_m \cdot \lambda_{ji}}{E_j \cdot I_{mr} \cdot A_{ji} \cdot g_j \cdot \lambda_{mr}}\right)} \quad (1)$$

Where: E is the energy level, KB is the Boltzmann constant, I is the spectral line intensity, A is the transition probability, g is the statistical weight and λ is the wavelength. These values can be found at the (NIST, 2010), except for the intensity, given by the sensor.

2.1.1 Change detection

The key idea behind change detection techniques is given by its name. It is to evaluate a signal and if there is an appreciable change in its behavior (frequency, magnitude or abrupt peaks), the system must be capable of detecting it. These perturbations can be defects on the welding process and a schematic diagram is given in Figure 2 (Gustafsson, 2000).

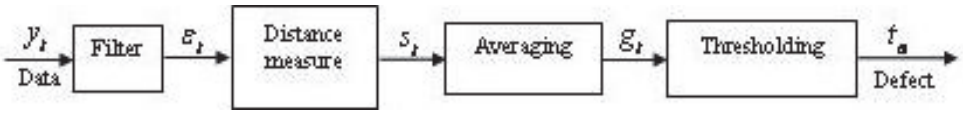

Fig. 2. Change detection diagram flux.

The blocks are explained separately. However, it is important to present the applied model first. The model proposed for the spectrometer reading is showed in Equation 2.

$$y_t = \theta_t + v_t \quad (2)$$

The signal given by the sensor (yt) is the radiation emitted by the plasma (θt) added by a noise (νt). The noise is a random variable with normal distribution with zero mean and variance R. Firstly, there is the filter block. It estimates the radiation intensity (θt) found in the reading model, Equation 2, and calculates the residual (εt). The next block calculates the distance. It is the difference between the sensor reading and the estimation. It is based on the residuals or it can be the value itself. A statistic test (gt) based on the distance is given in the third block. Finally, gt is compared to a threshold (h) to decide if there is a disturbance in the plasma. If the value is lower than the reference, it is assumed that the welding process is normal. Although, if the statistic test value is greater than the threshold, it is possible that a defect had occurred.

There are many change detection algorithms. It will present three of them. One widely used, Cusum LS Filter (Gustafsson, 2000), other developed by (Appel, 1983) and another here proposed, which applies steps from different algorithms. The Cusum LS Filter, Equation 3, presents a Least Square filter to estimate the radiation intensity, $\hat{\theta}_t$. The distance, s_t, is given by the residuals, ε_t, and the statistic test, g_t, is given by a cumulative sum. The factor σ is subtracted at each time instant t to avoid false alarms. Its value is chosen by the designer. And finally, the comparison of the statistic test to a threshold h. If its value is greater than h, an alarm is set and its instant, t_a, is recorded, the statistics tests are reset and t_0 becomes t. The input parameters are h and σ. With the values of the alarm instants, it is possible to indicate the defects position, once the weld speed is constant.

$$\begin{array}{ll} \textit{Filter} & \text{Distance } \textit{measure} \\ \hat{\theta}_t = \dfrac{1}{t-t_0} \cdot \sum_{k=t_0+1}^{t} y_k & \varepsilon_t = y_t - \hat{\theta}_{t-1} \end{array} \tag{3}$$

$$\begin{array}{ll} & \textit{Thresholding} \\ \textit{Averaging} & \\ g_t^{(1)} = \max\left(g_{t-1}^{(1)} + s_t^{(1)} - \sigma, 0\right) & \textit{if} \quad g_t^{(1)} > h \quad \textit{or} \quad g_t^{(2)} > h \quad \begin{cases} \textit{alarm}: \ t = t_a \\ g_t^{(1)} = g_t^{(2)} = 0 \\ t_0 = t \end{cases} \\ g_t^{(2)} = \max\left(g_{t-1}^{(2)} + s_t^{(2)} - \sigma, 0\right) & \end{array}$$

The other algorithms are based on sliding windows. There are two different proposals. A scheme can be seen in Figure 3. One proposal, first scheme, presents the idea to compare two models (two filters). Both models present the notation of Equation 2. The slow filter, that estimates M1, uses data from a very large sliding window. The fast filter estimates M2 by a small window. Then, two estimates, $\hat{\theta}_1$ and $\hat{\theta}_2$ with variances $\hat{R}_1$ and $\hat{R}_2$, are obtained. If there is no abrupt change in the data, these estimates will be consistent. Otherwise, an alarm is set.

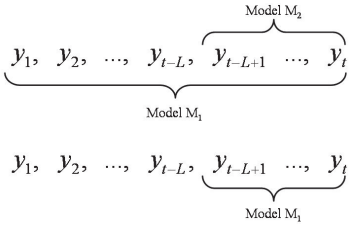

Fig. 3. Schemes for sliding windows.

An algorithm that adopts this scheme is the Brandt's GLR, proposed by (Appel, 1983). The algorithm is given by Equation 4. The variable $\hat{\theta}$ is the estimation of θ, L is the size of the sliding window, $\hat{R}$ is variance estimation and ta is the alarm time instant. Input parameters are L, h and, if the estimations do not converge, R_1 and R_2.

The other proposal, given by the second sliding window scheme, presents two Kalman Filters, Equation 5. One filter estimates the data in a sliding window, Model M_1 and the other estimates the past data at time t-1, Model M_2. The factor K is the filter gain and the Ps is the covariance matrix. For the distance measurement it was chosen the Brandt algorithm, Equation 4. The statistic test and thresholding are based in the CUSUM LS Filter, Equation 3. The algorithm parameters input are h, σ and R.

$$\begin{array}{ll} \text{Filter - Model M1} & \text{Filter - Model M2} \\ \hat{\theta}_t^{(1)} = \dfrac{1}{t-t_0} \cdot \sum_{k=t_0+1}^{t} y_k & \hat{\theta}_t^{(2)} = \dfrac{1}{t-L} \cdot \sum_{k=L+1}^{t} y_k \\ \hat{R}_t^{(1)} = \dfrac{1}{t-t_0} \cdot \sum_{k=t_0+1}^{t} \left(y_k - \hat{\theta}_t^{(1)}\right)^2 & \hat{R}_t^{(2)} = \dfrac{1}{t-L} \cdot \sum_{k=L+1}^{t} \left(y_k - \hat{\theta}_t^{(2)}\right)^2 \end{array} \tag{4}$$

Distance Measure

$$\varepsilon_t^{(1)} = y_t - \hat{\theta}_{t-1}^{(1)} \qquad s_t = \log\left(\frac{\hat{R}_t^{(1)}}{\hat{R}_t^{(2)}}\right) + \frac{\left(\varepsilon_t^{(1)}\right)^2}{\hat{R}_t^{(1)}} - \frac{\left(\varepsilon_t^{(2)}\right)^2}{\hat{R}_t^{(2)}}$$

$$\varepsilon_t^{(2)} = y_t - \hat{\theta}_{t-1}^{(2)}$$

Averaging

$$g_t = g_{t-1} + s_t$$

Thresholding

$$if \quad g_t > h \begin{cases} alarm: \quad t = t_a, \quad t_0 = t \\ g_t = 0 \end{cases}$$

Window Model M1 (5)

$$\varepsilon_t^{(1)-} = y_{t-L} - \hat{\theta}_{t-1}^{(1)} \qquad \varepsilon_t^{(1)} = y_t - \hat{\theta}_t^{(1)-}$$

$$K_t^{(1)-} = \frac{P_{t-1}^{(1)}}{P_{t-1}^{(1)} - R} \qquad K_t^{(1)} = \frac{P_t^{(1)-}}{P_t^{(1)-} + R}$$

$$\hat{\theta}_t^{(1)-} = \hat{\theta}_{t-1}^{(1)} + K_t^{(1)-} \cdot \varepsilon_t^{(1)-} \qquad \hat{\theta}_t^{(1)} = \hat{\theta}_t^{(1)-} + K_t^{(1)} \cdot \varepsilon_t^{(1)}$$

$$P_t^{(1)-} = \left(1 - K_t^{(1)-}\right) \cdot P_{t-1}^{(1)} + Q_1 \qquad P_t^{(1)} = \left(1 - K_t^{(1)}\right) \cdot P_t^{(1)-} + Q_1$$

Model M2

$$\varepsilon_t^{(2)} = y_t - \hat{\theta}_{t-1}^{(2)}$$

$$K_t^{(2)} = \frac{P_t^{(2)}}{P_t^{(2)} + R}$$

$$\hat{\theta}_t^{(2)} = \hat{\theta}_{t-1}^{(2)} + K_t^{(2)} \cdot \varepsilon_t^{(2)}$$

$$P_t^{(2)} = \left(1 - K_t^{(2)}\right) \cdot P_t^{(2)} + Q_2$$

Distance measure

$$s_t = \frac{\left|\varepsilon_t^{(1)} - \varepsilon_t^{(2)}\right|}{\sigma} = \frac{\left|\hat{\theta}_t^{(1)} - \hat{\theta}_t^{(2)}\right|}{\sqrt{P_t^{(1)} + P_t^{(2)}}}$$

Thresholding

$$if \quad s_t > h, \quad alarm: \quad t = t_a$$

Figure 4 shows the results of the experiment based on the variation of the shielding gas flow rate for the CUSUM LS Filter algorithm, the Figure 5 shows for the proposed algorithm and Figure 6 for Brand Algorithm. The welding parameters chosen were the industrial standard ones. The spectral line chosen was Argon 460.9 nm. The algorithms were capable of detecting fine changes. The ellipses indicate where initially the rate had changed.

The results suggest that a spectrometer can be applied as a sensor for detecting disturbances in the electric arc during welding. These disturbances can be related to weld defects. The radiation emission was analyzed instead of the electronic temperature, once the interest was only in signal changes, not in its absolute value. Bearing that in mind, the computational effort is lower. The change detection technique can be applied to point out disturbances in the sensor signal. The algorithms chosen to analyze the signal with the selected spectral lines presented satisfactory performances; the best being obtained using the CUSUM LS Filter was for gas flow variation. Other parameters and different elements (or ion) wavelengths can be applied. More than one spectral line can be monitored with different algorithm input parameters to ensure disturbance detection. The selection of the spectral line to be

monitored depends on the welding process, weld parameters, weld material and defects or disturbances to be monitored. Using this system, only the regions indicating defects will have to be inspected and reworked, therefore, shorter working hours and lesser consumables will be requiring, thus reducing production costs.

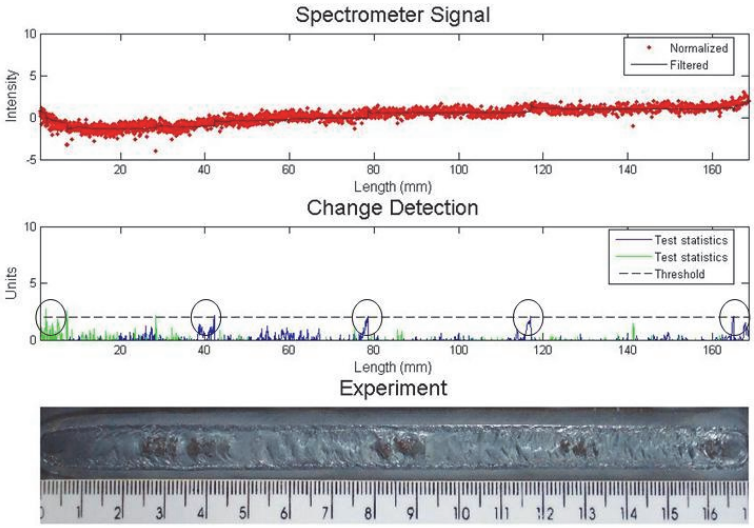

Fig. 4. Gas flow variation – CUSUM LS Filter.

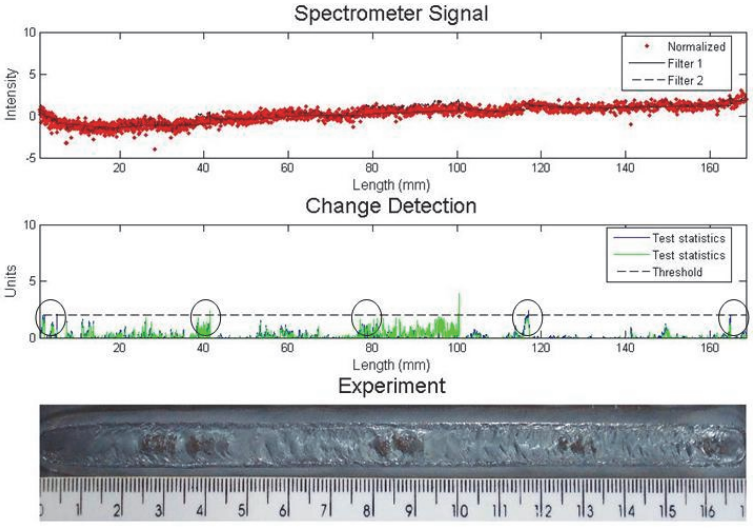

Fig. 5. Gas flow variation – proposed algorithm.

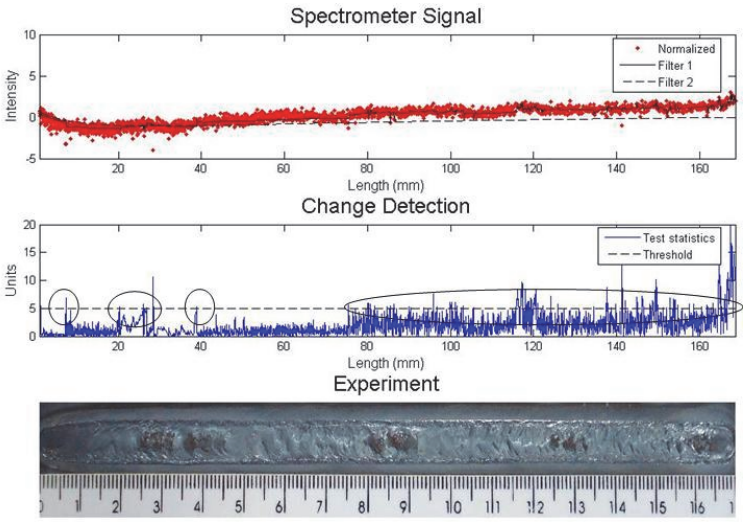

Fig. 6. Gas flow variation – Brandt algorithm.

2.2 Infrared monitoring

During the welding process, the high temperature associated with the arc and appropriate thermo physical properties such as thermal diffusivity cause strong spatial temperature gradients in the region of the weld pool. Convection in the weld pool, the shape of the weld pool and the heat transfer in both the solid and liquid metal determine the temperature distributions in the plate and on the surface. For an ideal weld with stable conditions, these surface temperatures should present repeatable and regular patterns. Perturbations in welding penetration should be clearly identifiable from variations in the surface temperature distribution (Nagarajan et al, 1989).

Infrared emissions indicate the heat content of the weld. For example, deeper penetration tends to correlate with increased heat input (caused by higher current or slower weld speed). Greater heat input results in higher temperatures and increased infrared emissions (Sanders et al., 1998). The temperature may be monitored by a pyrometer, but depend on the kind of sensor is using, due to the slow response time of the system and the presence of an intense thermal signal from the welding focused area (saturation problems). According to (Sanders et al., 1998), a better indicator is the infrared energy emitted by the weld, including both the contributions from the weld pool and plasma.

It is necessary to carry out the temperature measurement with a sensor that doesn't introduce defects during the welding process. It is for this reason that non-contact temperature sensors are more suitable. An infrared thermometer measures temperature by detecting the infrared energy emitted by all materials which are at temperatures above absolute zero, (0 Kelvin). Arc welding is intrinsically a thermal processing method. To this end, infrared sensing is a natural choice for weld process monitoring. Infrared sensing is a non-contact measurement of the emissions in the infrared portion of the electromagnetic spectrum.

The infrared monitoring techniques for weld pool are: area scanning and point monitoring. Area scanning provides a bidimensional view of the surface temperature distribution profile, making possible a complete analysis of the heat transfer process during welding (Nagarajan, 1989; Chen, 1990). Considering that we are dealing with bidimensional images, the application of area scanning demands a better computational structure (hardware and software), requiring a longer processing time (Venkatraman et al., 2006). On the other hand, the point monitoring technique demands little computational structure, requiring a shorter processing time, which makes it more appropriate for controlling in real time (Chin, 1999; Wikle, 2001). A recent study presented the adaptive control of welding through the infrared monitoring of the weld pool using point sensors (Araújo, 2004). The most basic design consists of a lens to focus the infrared (IR) energy on to a detector, which converts the energy to an electrical signal. This configuration facilitates temperature measurement from a distance without contact with the object to be measured (Merchant, 2008).
To make a correct measurement with this class of sensors, it is necessary to focalize the area that is going to be measured; this is possible by knowing the focal distance of the lens. Figure 7 shows a focal distance for one infrared sensor. In this case, a focal distance has a length of 600 mm and a radius of 4 mm (waist radius).

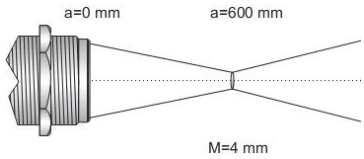

Fig. 7. TL-S-25 Infrared Sensor focus[1].

2.2.1 Failure detection

This study compares two algorithms for defect detection. The first one used is the conventional Kalman filter together with the Mahalanobis distance calculus to evaluate the presence of failures. In the second, the linear regression Kalman filter–LRKF and the generalized likelihood ratio test (Appel et al., 1983) are used to determine the distance between the autoregressive model and the signal read.

2.2.2 Change detection

This is a statistical technique that can detect abrupt changes in signals. Since welding is a stochastic process (Alfaro, 2006), some properties and algorithms can be applied. It consists basically on the flux of Figure 2.
Under certain model assumptions, adaptive filters take the measured signals and transform them to a sequence of residuals that results in a white before the change occurs (Gustafsson, 2000). If there is no change in the system and the model is correct, then the residuals are a sequence of independent variables with zero mean and known variance. When a change occurs, it can reflect on some variation in the mean, variance or both values that makes the residuals greater. The main point is to establish how great is this value to assume that a change had occurred. The statistical test decides whether the deviation is significant or not. The evaluation is usually made on four situations, change in the mean, change in the

[1] Calex Electronics Ltd

variance, change in correlation and change in signal correlation. In this work the evaluation was made on the mean and it is based on the residuals.
The stopping rule is based on the distance measurement. Many change detection algorithms make a decision between two hypotheses:

$$\begin{aligned} H_0 &: E(s_t) = 0, \\ H_1 &: E(s_t) > 0 \end{aligned} \tag{6}$$

This rule is achieved by the value calculated by the low-pass filter s_t and compares to a threshold. If the value is greater, an alarm is set.

2.2.3 Kalman filter

A simple description of the infrared signal behavior as a discrete temporal series can be made in terms of an autoregressive model (AR) of order m. The present sample value is represented by the linear combination of m past samples incremented by a parameter of uncertainty. For a temperature registry of a component z[t], According to (Pollock, 1999) the model AR of order m is given by Equation (7):

$$Z[t] = \sum_{i=1}^{m} a_i z[t-i] + \varepsilon[t] \tag{7}$$

where ai = {a1, . . . , am} are the coefficients of model AR and ε[t] is the noise component to represent the inaccuracy of the signal reading during welding. It is supposed that the sequence ε[1 : t] = {ε [1], ..., ε [t]} is independent and identically distributed (i.i.d) Gaussian with mean E{ε [n]} = 0, variance E{(ε[n])2} = σ2.
From the observation of different statistic characteristics in the noise residues and the presence of defect in a model AR of order m, it is possible to establish a recursive estimation system using a stochastic filtration technique to observe and track the temperature interval in which the gaussianity of the sequence is preserved. One of these tools is the Kalman filter. The state vector is given by Equation (8) (Jazwinski, 1970):

$$x[k] = A[k]x[k-1] + w[k] \tag{8}$$

where x[k] is the state vector of dimension n, A[k] is a square matrix of state transition, w[k] is a sequence of dimension n of Gaussian white noise of null mean. The observation model is given by Equation (9):

$$z[k] = H[k]x[k] + v[k] \tag{9}$$

in which z[k] is the observation vector of dimension m, H[k] is the measuring matrix and v[k] represents Gaussian white noise of null mean. It is supposed that the w and v processes are non-correlated and also:

$$\begin{aligned} E\{w[k]w[i]^T\} &= \begin{cases} Q[k], & if \quad k = i \\ 0, & if \quad k \neq i \end{cases} \\ E\{v[k]v[i]^T\} &= \begin{cases} R[k], & if \quad k = i \\ 0, & if \quad k \neq i \end{cases} \end{aligned} \tag{10}$$

In this system, the initial state $x[0]$ is a random Gaussian variable of mean $\hat{x}[0]$ and matrix of covariance P[0]. $x[0]$ is supposedly non-correlated to the w and v processes. The basic problem of the Kalman filter is to obtain an estimation $\hat{x}[k|k]$ of $x[k]$ from the measurement {z[1], z[2], . . . , z[k]}, in order to minimize a metric of mean square error. This metric is given by the trace of the *a posteriori* error covariance matrix as presented in Equation (11):

$$P[k|k] = E\left\{(x[k] - \hat{x}[k|k])(x[k] - \hat{x}[k|k])^T\right\} \tag{11}$$

Fortunately, this estimation problem presents a recursive solution. This solution is given in two stages. First there is a prediction stage (between observation Equation (12, 13)), in which:

$$\hat{x}[k|k-1] = A[k]\hat{x}[k-1|k-1] \tag{12}$$

$$P[k|k-1] = A[k]P[k-1|k-1]A[k]^T + Q[k] \tag{13}$$

Then, there is the correction stage in which the actual observation is used to correct the prediction $\hat{x}[x|k-1]$:

$$\hat{x}[k|k] = \hat{x}[k|k-1] + H[k](Z[k] - H[k]\hat{x}[k|k-1]) \tag{14}$$

$$P[k|k] = P[k|k-1] - K[k]H[k]P[k|k-1] \tag{15}$$

in which:

$$K[k] = P[k|k-1]H[k]^T\left[H[k]P[k|k-1]H[k]^T + R[k]\right]^{-1} \tag{16}$$

is named Kalman gain.

The main idea concerning the defect identification is related to the use of a statistic test that, jointly with stochastic filtration, verifies if the infrared samples properties are related to the estimation of the model AR given by the Kalman filter. If the test fails, it is supposed that the actual sample correlates with the presence of defect.

The comparison between the infrared signal sample and the recursive estimation consists in the Chi-square probabilistic hypothesis through the Mahalanobis distance (Duda, 2001). Such a distance is a natural measurement that indicates, in a probabilistic sense, how much of the registry of the actual sample is compatible with the estimated infrared signal model, estimated by the Kalman filter.

Figures 8 and 9 show an experiment in which the defects were introduced through the presence of water during the welding process. Figure 8 shows an analysis done with the generalized likelihood ratio test, and Figure 9 shows an analysis done according to the Mahalanobis distance. In Figure 8 we observe four clearly detected defects, it is observed that the last two defects remained on the limit of the Stopping Rule and two more anomalies were detected around 108 and 110 mm. In just one of them (108 mm) a variation in the form of a bead is observed.

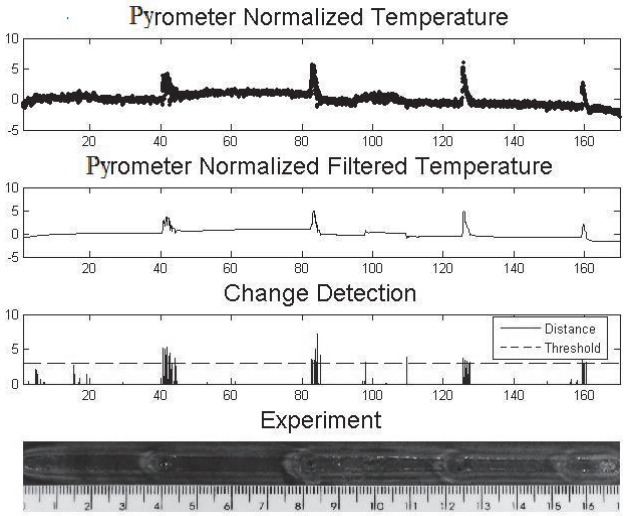

Fig. 8. Plate with water defects and change detection analysis.

Figure 9 shows an analysis according to the Mahalanobis distance. It is observed that the distance to the region where there is no presence of defects (constant temperature) is located below the threshold proposed by the statistic test. During the presence of the defect, the residue between the real sample Z[k] and the sample estimated by the AR coefficient increases at such a rate that the distance Z[k] surpasses the established threshold where the defect presence is verified. We should also note that this test could not detect the anomalies presented around 105 mm.

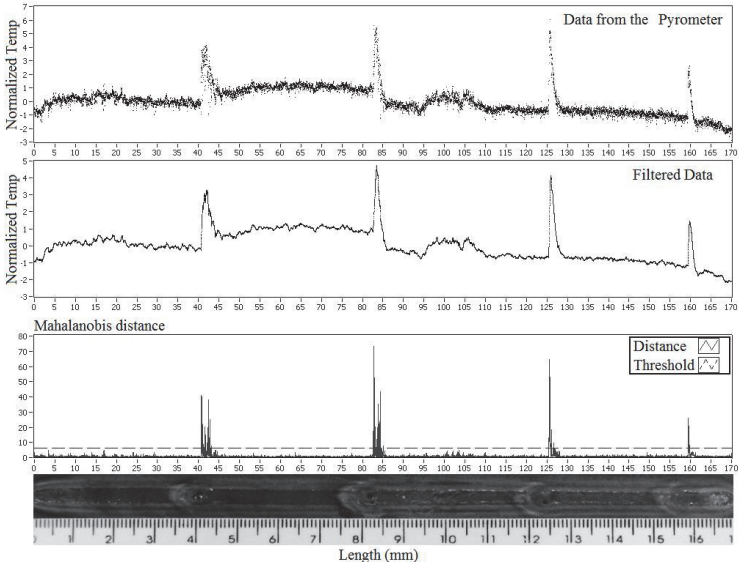

Fig. 9. Current Plate with water defects and Mahalanobis distance.

Infrared weld pool monitoring in the GTAW process provides information about penetration depth. It also shows that infrared signal variations in DC are related to weld penetration depth, while AC portions of the output can be correlated with surface irregularities.
Together with a change detection algorithm, the system monitors the residual of the regression algorithm, looking for changes in the mean. The proposed method maintains a regression model where residuals are filtered by a Kalman filter. A Mahalanobis distance algorithm monitors significant changes in the output of the Kalman filter. The Kalman filter has a good performance in detecting real changes from noisy data. The simplicity of the proposed algorithm permits its implementation in systems for monitoring, detection and localization of events in real time.

2.3 Acoustic sensing

By monitoring arc voltage and welding current allowing the detection of the arc perturbations during the welding process and depending of its profile, these perturbations can be interpreted as defects on the welded joints. The on-line detection and localization of the defects reduces the severity and time consuming of the quality control tests. Most of the commercial equipment for arc voltage and welding current monitoring use sensors based in voltage divisors and Hall Effect and they are installed directly on the welding process. The sensors connected directly on the welding process present two considerable disadvantages: The stability on the welding process, due to its high sensibility, can be interfered by the sensors with electrical connections altering the electrical arc impedance and generates undesirable arc instabilities and the electromagnetic arc interferences alters considerably the measure makes by the sensors. The electrical arc generates physical phenomena like luminosity, infrared radiation electromagnetic fields and sound pressure. It is known that the specialized welders use an acoustic and visual combination for the monitoring and control of the welding process (Kralj et al., 1968). In the end 70 years' measurement of electrical arc voltage was successfully carried out by acoustical methods (Drouet, 1979, 1982). The welding arc sound represents the behavior of the electrical parameters of the welding arc, consequently this fact make possible monitoring the stability of the welding process through the sound. The arc sound of the GMA welding in the short circuit transfer mode can represent the extinction and ignition sequence of the arc voltage and therefore it opens the possibility to detect acoustically perturbations in the welding arc (Cayo, 2008). The main advantage of the sound monitoring system lies on the fact that there is no need to have electrical connections to the welding process since the sound is transmitted from the welding arc to acoustic sensor through the air. This fact make eases the installation of the sensor and reduces the possibility to alter the electric parameters of the welding process and reduces the influence of the electromagnetic field on the acoustic sensor. It can be found in literature some acoustical monitoring systems for GMA welding process, but it not yet are used in the industry (Mansoor, 1999; Grad, 2004; Poopat, 2006; Cayo, 2007). In the present work was developed a weld defect detection technique based on the welding stability evaluation through sound produced by welding electric arc.

2.3.1 Welding electrical arc and acoustical signals

The relationship between sound pressure, sound pressure level and spectrum frequency profile behavior with the arc voltage and welding current have been studied. The sound

pressure is a longitudinal mechanical wave, produced by the difference of pressure in a medium that can be solid, liquid or gaseous; in this work the transport medium is the air. The metallic transference in the welding process produces changes in the air volume on the electric arc environment. This change produces pressure variations that are airborne transported and sensing by the microphone. The sound pressure from electric arc is a consequence of amplitude modulation of arc voltage and welding current (Drouet, 1979, 1982). This relation is expressed by the equation (17).

The sound pressure level – SPL also called as equivalent continuous sound pressure level, is a comparative measurement with the microphone sensitivity. It is defined as twenty times the logarithm in base ten of the ratio of a toot-mean – square sound pressure during a time interval to the reference sound pressure. The equation (18) expresses the sensibility function.

$$S_a(t) = \frac{d(k.V(t).I(t))}{dt} \tag{17}$$

Where, *Sa (t)* is the sound signal (V), *V (t)* the arc voltage (V),
I(t) welding current (A) and *K* the geometric factor.

$$SPL = 20.Log\left[\sqrt{\frac{1}{\Delta t}\int_{t}^{t+\Delta t} P^2(\xi)d\xi}\Big/ p_o\right] \tag{18}$$

The relation between the microphone pressure response and its sensibility is given by the equation (19) and therefore the SPL in function of the sound pressure is given by the equation (20). Relating the equation (17) and (20) results the equation (21) that expresses the SPL in function of the arc voltage and welding current.

$$P(\xi) = \frac{S(\xi)}{50E-3} \tag{19}$$

$$SPL = 20.Log\left[\sqrt{\frac{1}{\Delta t}\int_{t}^{t+\Delta t}\left(\frac{S(\xi)}{50E-3}\right)^2 d\xi}\Big/ p_o\right] \tag{20}$$

$$SPL = 20.Log\left[20\sqrt{\frac{1}{\Delta t}\int_{t}^{t+\Delta t}\left(\frac{d(k*V(\xi)*I(\xi))}{d\xi}\right)^2 d\xi}\Big/ p_o\right] \tag{21}$$

In which SPL is the sound pressure level, V the arc voltage, I the arc current, K the geometrical factor, Po the reference sound pressure (20 uPa), ξ is a dummy variable of time integration over the mean time interval, t the start time of the measurement, Δt the averaging time interval, S the sound signal.

For the spectrum frequency profile analysis it has been used the continuous Fourier transform; it is a linear transformation that converts the acoustic pressure signal from time domain to frequency domain.

This transformation is made using the Discrete Fourier Transform - DFT and it is expressed by the Eq. 22.

$$S(k) = \frac{1}{N}\sum_{n=0}^{N-1} s(n)e^{-j2\pi kn/N} \tag{22}$$

The octave frequency fractions analysis allows to evaluate the frequency strips behavior instead of any frequency. A frequency octave is defined as an interval among two frequencies where one of them is the double of the other. The octave band limits are calculated by Eq. 23, to 25. After obtaining the acoustic pressure spectra S(k), is obtained the octave frequency strips G(n) from Eq. (26).

$$f_{C_{n+1}} = 2^m f_{C_n} \tag{23}$$

$$f_{L_n} = \frac{f_{C_n}}{2^{m/2}} \tag{24}$$

$$f_{U_n} = 2^{m/2} f_{C_n} \tag{25}$$

$$G(n) = \sqrt{\frac{1}{(f_{U_n} - f_{L_n})}\sum_{f(k)=f_{L_n}}^{f_{U_n}} [S(f)]^2} \tag{26}$$

Where m is the octave band fraction, f_{Cn} central frequency of the n band, f_{Ln} the inferior limit of the n band and f_{Un} the superior limit of the n band.

2.3.2 Quality control in the GMA welding process

The quality control study in the welding processes is a main subject of many researchers. The evaluation task of weld quality is not trivial, even for the experienced inspector. This is particularly true when it comes to specifying in quantitative terms what attributes of the weld affect its quality and in what extent. Different types of discontinuities have been categorized for this purpose, such as cracks, porosity, undercuts, microfissures, etc. (Cook, 1997). Generally, good quality GMA welds are uniform and contain little or no artifacts on the bead surface. Furthermore, the bead width is relatively uniform along the length of the bead (Cook, 1995). To reaches the standard weld quality is fundamental maintain continuity on the welding stability and this happens when the mass and heat flow of the end consumable electrode until fusion pool through arc maintains uniformity in the transference; possible discontinuities and/or upheavals in the transference could originate weld disturbances. The stability of the short circuit gas metal arc welding process is directly related to weld pool oscillations. Optimal process stability corresponds to maximum short-circuit rate, minimum standard deviation of the short-circuit rate, a minimum mass transferred per short circuit and minimum spatter loss, (Cook, 1997; Adolfsson, 1999; Wu, 2007). In the present work, the welding stability was evaluated using the sound pressure through the acoustic ignition frequency (AIF) and sound pressure level (SPL) signatures.

The metallic transference on the short circuit mode in GMA welding (GMAW-S[2]) is characterized by a sequence cycles of ignition and extinction arcs. The Figure 10 - a show the behavior of arc welding current and voltage signals as well as the welding arc sound and

[2] Gas Metal Arc Welding in short circuit transfer mode

the resultant signal using the equation (1). The sequence cycles of the welding metallic transference is replicated in the electrical measured signal as well as in the welding arc sound. The arc ignition produces a great acoustical peak and the arc extinction produces a small amplitude acoustical peak. Although, it is possible to observed a delay 'Δt' on the similarity signal of calculated and measured arc sound (see Fig. 10 - b). Some studies in psychoacoustic have determined that while the delay of welding arc sound signal does not exceed 400 ms, the sound will be a good indicator of welding process behavior (Tam, 2005). In our case the Δt delay measured was approximately 0,6 ms, this value undertakes the reliability to monitoring the welding process behavior.

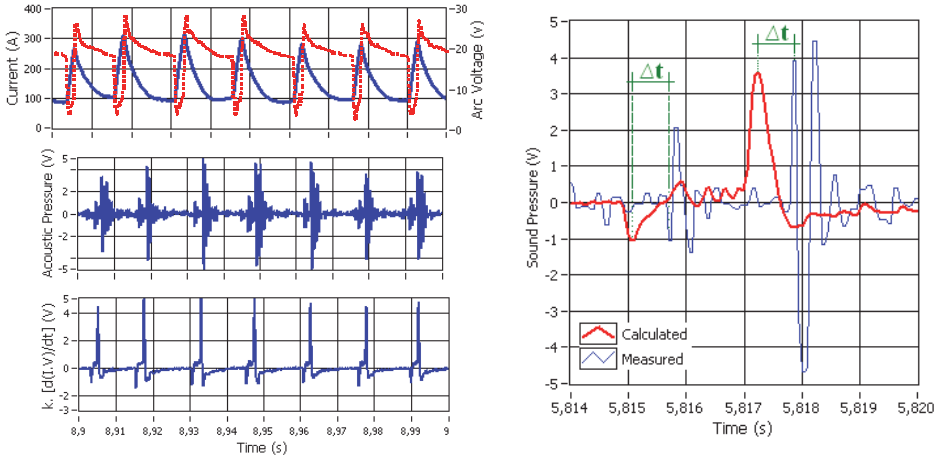

a) b)

Fig. 10. (a) Welding Signals (b) Sound pressure calculated and measured.

The welder uses his experience and ability to learn and know acoustical signatures from quality welds. The figure 11 shows the measured and calculated SPL (using the equation 5) with its respectively sound pressure signal. It can be observed that the shielding gas flux is sensed by the sound signal, but as the SPL calculated is only function of welding current and arc voltage, this sound signal is not taking into the account. It can be obtained others information from the SPL sound pressure like the arc welding ignition and extinction average frequency, the average period of the transferences cycles and its standard deviations.

The measurement of ignition and extinction average frequency from welding arc is a method for evaluate welding stability (Adolfsson, 1999). As it was explained before, the arc sound pressure follows the arc ignition and extinction sequence (Fig. 10 - b). The acoustic amplitude pulses produced by the arc ignitions are greater than acoustic amplitude pulse produced by the extinctions (short circuits). These acoustical impulses sequence occurs together with chaotic transients and noise oscillations and in order to reduces it and to obtain only the ignition and extinction average frequency, the envelope sound signal was extracted from acoustic sound signal (see Fig. 12).

The envelope sound signal was obtained using a quadratic demodulator. Squaring the signal effectively demodulates the input by using itself as the carrier wave. This means that half the energy of the signal is pushed up to higher frequencies and half is shifted towards

DC. The envelope can then be extracted by keeping all the DC low-frequency energy and eliminating the high-frequency energy. However, the statistical filter called "kalman filter" was used due to the sound pressure have a stochastic behavior and were low-pass filters is needed with an elevated order, this order produce a pronounced delay and deformation in the envelopment signal. This statistical filter instead of letting pass low frequencies, it follows the statistical tendency of the squared signal obtaining in the envelopment sound pressure (Cayo, 2008). In Figure 12, the 150 ms moving window data was extracted from the sound pressure signal. From envelop sound pressure signal is calculated the arc ignitions for each moving window data. An ignition takes place whenever the envelop sound pressure signal surpasses the ignition threshold established (k = 0,2).

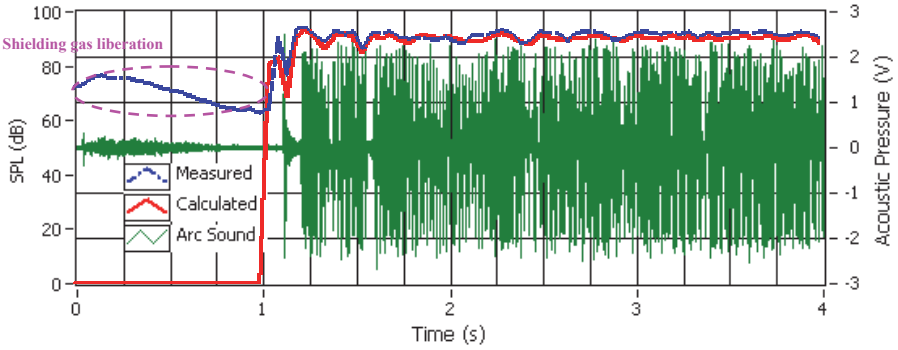

Fig. 11. Measured and Calculated SPL.

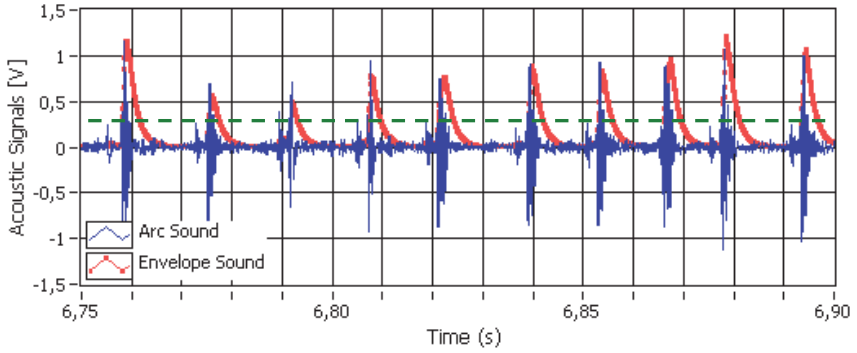

Fig. 12. Acoustical Pressure and its envelope Signals.

2.3.3 Weld bead quality profile identification

Previous to the interferences detection, many weld experiments for finding the optimal set of the welding parameters was carried out. The satisfactory parameters selection allows reaching the maximum stability in welding, but to reach that was necessary chooses the adequate arc voltage.

The figure 13 – a, illustrates the relationship between the short circuit frequency calculated by the arc voltage and arc sound and in figure 13-b is showed the respective standard deviation. The average short circuit frequency obtained from arc voltage and the arc sound pressure show a similar result. Moreover, in both short circuit frequency and standard deviation have some differences between calculating methods, but this differences are minimal and the acoustical method to calculate these statistical parameter can be considered as reliable. To choose the arc voltage value that generated the best quality bead (continuity and uniformity on the bead ruggedness) following related research (Adolfsson et al., 1999) that concluded that the best quality is reached basically when the short circuit rate is maximum and its standard deviation is minimal was discover some unexpected results. The arc voltage that generates the maximum short circuit rate (17,5 V) is not the weld with the better quality inside the weld run experiments (Fig. 12). Considering the arc voltage that generates the minimal standard deviation from short circuit rate obtained from arc voltage (23,0 V) is not the weld with the better quality and considering the minimal standard deviation obtained from arc sound also is not the weld with the better quality. The visual inspection of the bead set shows that the weld bead run with the voltage range between 19,0 V and 20,5 V can be considered as the best quality weld bead inside this set.

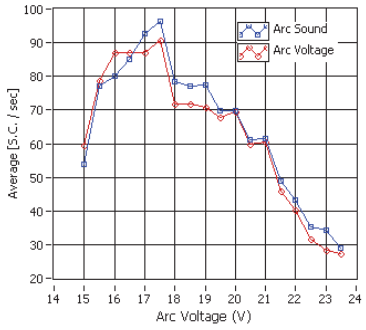

a) Short Circuits Frequency

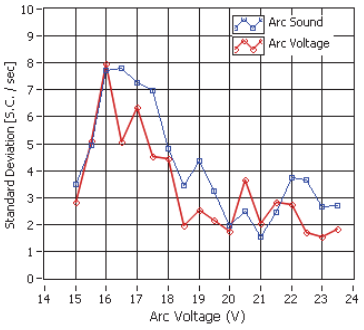

b) S. C. F. Standard Deviation

Fig. 13. Short Circuits vs Arc Voltage.

In order to chosen the arc voltage value that generates the best weld bead quality was carried out a second statistical analyze. The Figures 14 – a, illustrate the relationship between the transference cycle period average obtained by the arc voltage and arc sound at the same different arc voltage values analyzed previously. In this case the results obtained by the electrical and acoustical methods show a narrow similarity with differences of milliseconds. The arc voltage that generates the least transference cycle period average was also 17,5 and comparing with the weld bead quality shows not the best. The transference cycle period uniformity is measured by its standard deviation as show in the figure 14 – b. This standard deviation distribution has more uniformity than the short circuit frequency standard deviation and the arc voltage that generates the minimal value into standard deviation distribution (20,0 V) also generates the weld bead with more geometrical ruggedness and uniformity and can be considered as the best quality weld bead. Consequently, the remaining weld run experiment for interferences detection will carry out using the welding parameters showed in table 1 with arc voltage adjusted to 20,0 V.

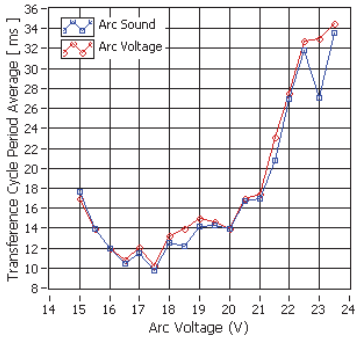

a) Short Circuits Frequency

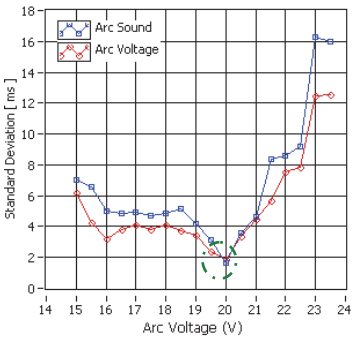

b) S. C. F. Standard Deviation

Fig. 14. Transference cycle Period .vs. Arc Voltage.

2.3.4 Acoustical profiles to interferences detection

The general approach used to evaluate GMA welds was examining the variation of weld profiles, sampled across the weld bead in a sequence of locations. A high quality weld would generally yield small variation in the weld profiles, while low quality weld profiles would vary substantially, as irregularities and various discontinuities are encountered in the distinct profile scans (Cook, 1997). The initial weld profiles tested were the arc sound ignitions frequency, the average sound pressure level and the power spectral density using the continuous and octave fraction frequency domain. The figure 15 – a, shows the AIF and 15 – b, the SPL weld profiles signal behavior. These profiles were tested on welding runs with and without presences of disturbances. Both profile signals were determined using a moving windows signal applied on the arc sound pressure signal. The moving window was fixed in 150 ms considering that the data sample rate was 20 kHz.

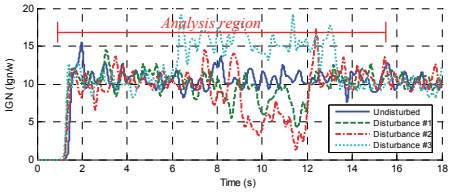

a) Ignition Frequency – AIF

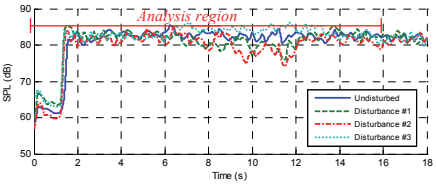

b) Sound Level Pressure - SPL

Fig. 15. Time Profiles to welding arc sound.

Signature analysis of the short-circuiting frequency by using time – frequency analysis method was applied to welding arc sound. On this signal there are two regions (undisturbed - UR and disturbed - DR regions). On these regions a spectral analysis was made at continuous and an octave fractions frequency. When the welding entered on the interfered region the spectra frequency varies its magnitude on the overall frequency. The spectra frequency magnitude varies on the two analyzed regions; there are approximately dominant frequency components at 2 kHz.

The octave fraction spectra also have greater amplitude inside this band frequency, but it does not show frequency bands signatures that vary pronouncedly to disturbed sound

signals. As there are not signature bands in fraction octave analysis, the continuous frequency versus time behavior was analyzed. The figure 10 shows the spectrogram for welding runs with induced interferences on the plate. The amplitude variations on the sound spectra imply that there are signature variations on the time domain. The welding arc sound have many chaotic transients between impulses, these fluctuation have a stochastic nature. Fourier analysis is very effective in problems dealing with frequency location. However, there are severe problems with trying to analyze transient signals using classical Fourier methods (Walker, 1997). This is the principal reason for not distinguishing clear signatures frequencies on the arc sound spectra that can identify disturbances. The signatures on the time domain describe in figure 15 shows pronounced signatures when the welding enters to interfered regions.

2.3.5 Interferences monitoring and detection

The disturbances detection was made using a limit control based on the third standard deviation method. This control shows optimal results in the disturbances detection of both, electric arc voltage and welding current monitoring signals (Cook, 1995, 1997). As already explain, the signature signals analysis was made on the 150 ms moving window. The equation (27), (28) and (29) represents the average, standard deviation and disturbances control limits for each moving window data respectively.

$$\overline{x_i} = \frac{1}{n}\sum_{j=1}^{n} x_i = \frac{1}{n}(x_1 + ... + x_n) \tag{27}$$

$$S_i = \sqrt{\frac{1}{n}\sum_{j=1}^{n}(x_j - \overline{x_i})^2} \tag{28}$$

$$Control\_Limits = \overline{P_N} \pm 3 \times S_P \tag{29}$$

Where:

$\overline{x_i}$ Average parameter of the *i* analysis moving windows (150 ms)
x_i data *i* from the moving window
n Data component number from analysis moving window
S_i The standard deviation for the *i* analysis moving window data,
$\underline{x_j}$ The j component data from analysis moving window data,
$\overline{P_N}$ Average established for each parameter,
S_P The standard deviation established for each acoustical parameter without

In order to validate the disturbances detection method and base on the acoustics GMAW-S signal, a total of forty welding runs were carried out. The average short circuit numbers per seconds obtained from arc voltage and the arc average ignition numbers per seconds obtained from sound pressure show a similar result as shown in figure 16 - a. These results were obtained in the first weld experiments group without induced disturbances. The minimal standard deviation 16 – b confirms that the arc sound pressure can well represent the behavior of the GMAW-S metallic transference.

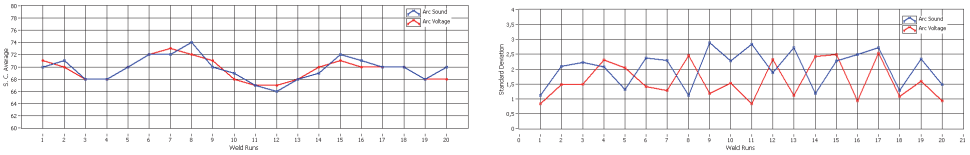

a) S. C. Average b) S. C. Standard Deviation

Fig. 16. Short circuits average and standard deviation.

The initial time profiles have temporarily instabilities [Figures 15 (a) and (b)]. In order to avoid these initial instabilities influence in the quality control evaluation, the analysis region is established from second 2 to second 18. From the figure 17 and 18, (a), (b) and (c) respectively, are showed the acoustical parameters behavior and it can also be observed a baseline and two threshold levels, one superior and another inferior. These established limits are three times the standard deviation on the average of each parameter in stable conditions welds (without the presence of disturbances). When the parameters are within these two threshold limits are no apparent disturbances in the welds. Therefore, when the parameters exceed the established threshold limits implies in having detected some disturbance that possibly could originate some weld defect. Figure 17 (a) and (b) show the AIF and the SPL behaviors, respectively obtained from the acoustical of arc without induced disturbances. In the Figure 17 (c) is showed the aspect of the welding bead and even appearing oscillations on the signal, it does not exceed the established threshold limits. These oscillations appear due to stochastic behavior of the acoustical pressure emitted by the electric arc of the welding process and do not necessarily represent disturbances presence.

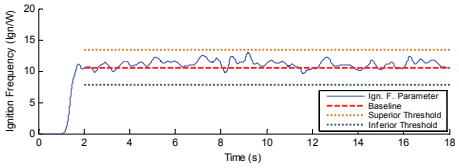

a) Ignition Frequency

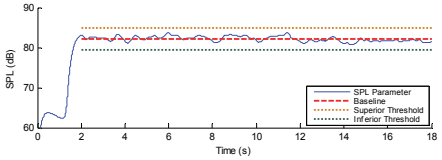

b) Sound Pressure Level

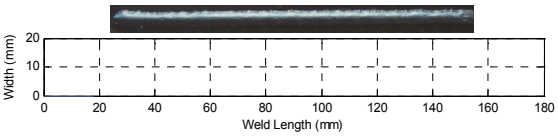

c) Weld Bead without Disturbance

Fig. 17. Parameters without Disturbance.

The Figure 18 (a) and (b) show the AIF and the average SPL per moving window respectively. Both graphics were obtained from the acoustics of a welding arc with induced disturbance originated by the arc length variation. The Figure 18 (c) shows the visual aspect of the weld bead. The instabilities only occurs when the weld bead pass through the beginning, end and the holes of the added plate, respectively. In Figure 18, (a) and (b) can also be observed that the ignitions frequency and the SPL do not present oscillations that exceed the established threshold limits, before and after the weld bead pass throughout the interference region. When the weld passage throughout the interference region, abrupt changes of signal level are produced in each parameter. These instabilities exceed the level control previously established. When the CTWD length varies, the arc length varies too, these variations produce instabilities in the arc ignition. It can also be observed that the parameters return to inside threshold limits even without leaving the disturbance region due to the arc reaches a new level of stability.

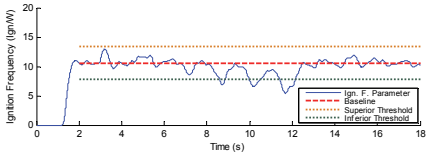

a) Ignition Frequency

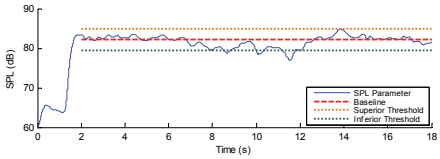

b) Sound Pressure Level

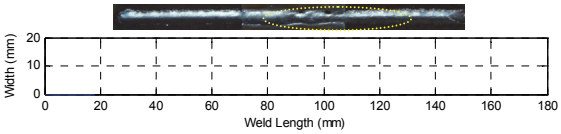

c) Weld Bead with Disturbance 1

Fig. 18. Parameters with disturbance.

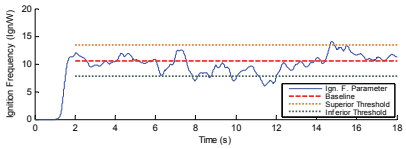

Fig. 19. a) Ignition Frequency

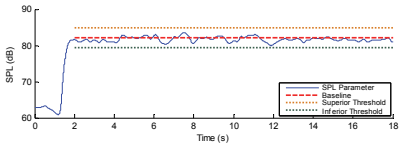

b) Sound Pressure Level

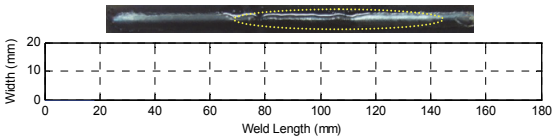

c) Weld Bead with Disturbance 2

Fig. 19. Parameters with Disturbance 2.

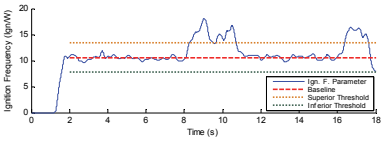

a) Ignition Frequency

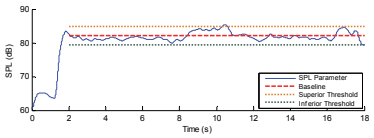

b) Sound Pressure Level

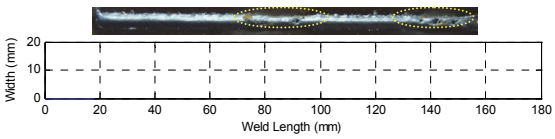

c) Weld Bead with Disturbance 3

Fig. 20. Parameters with Disturbance 3.

In the Figure 19 (a) and (b) is showed the acoustical stability parameters behavior for a weld bead with a disturbance induced due to grease presence in the welding trajectory (see Fig. 19-c). When the welding run pass the disturbance region, instabilities in the arc ignitions was observed and unexpected upheavals in the metallic transference cycles occurs forming weld bead deposit interruptions in all welding trajectory. Initially, when the weld run reach the grease do not take place oscillations in the ignition frequency due to the grease borders are evaporate caused by the thermal welding cycles. In the AIF parameter can be observed that the interference is noticeable as a chaotic decrement, however this behavior overcame

slightly the control limits (see Fig. 19-a). The average SPL parameter has little abnormal variations when the weld run pass on the interference. The induced interference generates structural discontinuities in weld bead but only in AIF parameter is most evident that the SPL parameter. The Figure 20 (a) and (b) show the AIF and SPL parameter behavior in welding experiment without shield gas. In this case the induced perturbations were localized in two regions on the weld bead. These interferences have led to porosities formation (see Fig. 20-c) and higher spatter level. The AIF parameter has incremented suddenly and this behavior is showed in both instabilities and exceeds the control limit established. The AIF were incremented because the absence of the shield gas causes contamination in the arc welding environment originating the incomplete metallic transference, increasing the short circuit and ignitions rate. This increment noticeable in the AIF is also noticeable in the SPL, nevertheless these variations do not exceed the threshold limit control.

3. Conclusions

Signals of the arc voltage and sound pressure were tested for monitoring the welding process. As both signal have the same behavior, it can be concluded that the sound pressure can be used for welding monitoring. From sound pressure were calculated two parameters: AIF and SPL. The monitoring of the GMAW-S process by digital analysis of acoustical welding parameters enable to detect disturbances related to phenomena that take place in welding arc and can influence its stability. This fact shows that the arc acoustics is a non-intrusive potential tool that could be used for the weld quality evaluation.

4. References

Adolfsson, S.; Bahrami, A.; Bolmsjö, G.; Claesson, I. On-line quality monitoring in short-circuit gas metal arc welding Weld. J. 1999, 3, 59s–73s.

Alfaro, S., D. Mendonça, M. Matos, "Emission Spectrometry evaluation in arc welding monitoring system", Journal of Materials Processing Technology, No. 179, 2006, Pages 219-234.

Alfaro, S., P. Drews, "Intelligent Systems for Welding Process Automation", Journal of the Brazilian Society of Mechanical Sciences, Vol. 28, No. 1, 2006, Pages 25-29.

Alfaro, S.C.A.; Carvalho, G.C.; Da Cunha, F.R. A statistical approach for monitoring stochastic welding processes. J. Mater Process Technol. 2006, 175, 4–14.

Appel, U.; Brandt, A.V. Adaptive sequential segmentation of piecewise stationary time series. Inform. Science 1983, 29, 27–56.

Araújo, C.F.B. Estudo da Monitoração por Infravermelho como Indicador de Penetração em Soldas Obtidas no Processo TIG. Masters Dissertation, University of Brasilia: Brasilia, Brasil, 2004.

Cayo, E., S. Alfaro, "Welding Quality Measurement Based On Acoustic Sensing", COBEM-2007, Brasília. 19th International Congress of Mechanical Engineering. São Paulo : ABCM, 2007. v. 1. Pages 2200

Cayo, E. H.; Alfaro, S.C.A. Medición de la Calidad en Soldadura Basado en Sensoreamiento Acústico. In 8th Congreso Iberoamericano de Ingeniería Mecánica: Cuzco, PE, October 2007, pp.1068-1079.

Cayo, E., "Monitoring, Detection and Localization System for Welding Defects based on the Acoustic Pressure of the GMAW-S Process Electric Arc". Master Dissertation in Mechatronics Systems, FT, The University of Brasilia, DF, Brazil, 2008, Pages 108.

Cayo, E. H. Monitoring, Detection and Localization System for Welding Defects based on the Acoustic Pressure Electric Arc of the GMAW-S Process Master Dissertation in Mechatronics Systems, FT University of Brasilia, DF, Brazil, 2008.

Cayo, E., S. Alfaro, "GMAW process stability evaluation through acoustic emission by time and frequency domain analysis", AMME' 2009, June 2009, Gliwice, Poland, 2009, p. 157-164.

Chen, W.; Chin, B.A. Monitoring Joint Penetration Using Infrared Sensing Techniques. Weld J. 1990, 69, 181s–185s.

Chin, B.A.; Zee, R.H.; Wikle, H.C. A Sensing System for Weld Process Control. J. Mater. Process. Technol. 1999, 89–90, 254–259.

Cook, G.E.; Barnett, R.J.; Andersen, K.; Springfield, J.F.; Strauss, A.M. Automated Visual Inspection and Interpretation System for Weld Quality Evaluation, Thirtieth IAS Annual Meeting, IAS '95, Conference Record of the 1995 IEEE: Orlando, FL, USA, October 1995; pp.1809 -1816.

Cook, G.E.; Maxwell, J.E.; Barnett, R.J.; Strauss, A.M. Statistical Process Control Application to Weld Process, IEEE Transactions on Industry Applications 1997, 33, No. 2, 454s-463s.

Drouet, M.; Nadeau, F. Pressure waves due to Arcing Faults in a Substation, IEEE Transactions on Power Apparatus and Systems 1979, 5, 98s.

Drouet, M.; Nadeau, F. Acoustic measurement of the arc voltage applicable to arc welding and arc furnaces Phys J. 1982, 15, 268s-269s.

Duda, R.O.; Hart, P.E.; Stork, D.G. Pattern Classification; 2nd ed. John Wiley and Sons, Inc.: New York, NY, USA, 2001.

Fan, H., N. Ravala, H. Wikle III, B. Chin, "Low-cost infrared sensing system for monitoring the welding". Journal of Materials Processing Technology, no. 140, 2003, Pages 668-675.

Fortunko, C.M. Ultrasonic Detection and Sizing of Two-Dimensional Weld Defects in the Long-Wavelength Limit. Ultrason. Symp. 1980, 862–867.

Grad, L., J. Grum, I. Polajnar, J. Slabe, "Feasibility study of acoustic signals for on-line monitoring in short circuit gas metal arc welding", International Journal of Machine Tools and Manufacture Volume 44, Issue 5, April 2004, Pages 555-561.

Gustafsson, F. Adaptative Filtering and Change Detection; John Wiley & Sons: New York, NY, USA, 2000.

Jazwinski, A.H. Stochastic Processes and Filtering Theory; 1st ed.; Academic Press: New York, NY, USA, 1970.

Kerr, H.W.; Hellina, M.C.; Huissoon, J.P. Identifying Welding Pool Dynamics for GMA fillet welds. Scien. Tech. Weld. Join. 1999, 4, 15–20.

Kralj, V. Biocybernetic investigations of hand movements of human operator in hand welding. Int. Ins. Weld. 1968, Doc. 212-140-68,

Lacroix, D., C. Boudot, G. Jeandel, "Spectroscopy Studies of GTA Welding Plasmas. Temperature Calculation and Dilution Measurement". Euro Physics Journal, AP 8, 1999, Pages 61-69.

Liu, Y.; Li, X.H.; Ren, D.H.; Ye, S.H.; Wang, B.G.; Sun, J. Computer vision application for weld defect detection and evaluation, Automated Optical Inspection for Industry. Theory Technol. Appl. II. 1998, 3558, 354–357.

Luo, H.K.; Lawrence, F.M.K.; Mohanamurthy, P.H.; Devanathan, R.; Chen, X.Q.; Chan, S.P. Vision Based GTA Weld Pool Sensing and Control Using Neurofuzzy Logic; SIMTech Technical Report AT/00/011/AMP; Automated Material Processing Group: Singapore Institute of Manufacturing Technology, Singapore, 2000, 1–7.

Mansoor, A., J. Huissoon, "Acoustic Identification of the GMAW Process", 9th Intl. Conf. on Computer Technology in Welding, Detroit, USA, 1999, Pages 312-323.

Marotta, A. (1994), "Determination of axial thermal plasma temperatures without Abel inversion", Journal of Physics D. Applied Physics, 27, 268-272.

Merchant, J. Infrared Temperature Measurement Theory and Applications, Mikron Instruments Company Inc, Application Notes, 2008.

Mirapeix, J.; Cobo, A.; Conde, O.M.; Jaúregui, C.; López-Higuera, J. M. Real-time arc welding defect detection technique by means of plasma spectrum optical analysis. NDT&E Int. 2006, 39, 356–360.

Mirapeix, J., A. Cobo, D. González, J. López-Higuera, "Plasma spectroscopy analysis technique based on optimization algorithms and spectral synthesis for arc-welding quality assurance". Optics Express, Vol. 5, no. 4, 2007, Pages 1884-1889.

Nagarajan, S.W.; Chen, H.B.; Chin, A. Infrared Sensing for Adaptive Arc Welding. Weld J. 1989, 68, 462s–466s.

Nagarajan, S., P. Banerjee, W. Chen, B. Chin, "Control of the Process Using Infrared Sensors", IEEE Transaction on Robotics and Automation, Vol. 8, no. 1, 1992, Pages 86-93.

NIST, National Institute of Standards and Technology (accessed in may 2010) http://physics.nist.gov/PhysRefData/ASD/lines_form.html

Pollock, D.S.G. A Handbook of Time Series Analysis, Signal Processing and Dynamics; 1st ed.; Academic Press: New York, NY, USA, 1999.

Poopat, B., E. Warinsiriruk, "Acoustic signal analysis for classification of transfer mode in GMAW by noncontact sensing technique", Journal of Science and Technology, University of Technology Thonburi, Thungkru, Bangmod, 2006, Bangkok, Thailand, Vol. 28, Issue 4, Pages 829-840.

Sanders, P.G.; Leong, K.H.; Keske, J.S.; Kornecki, G. Real-time Monitoring of Laser Beam Welding using Infrared Weld Emissions. J. Laser Appl. 1998, 10, 205–211.

Tam, J., "Methods of Characterizing Gas-Metal Arc Welding Acoustics for Process Automation", Master Dissertation in Mechanical Engineering, University of Waterloo, Canada. 2005, Pages 120.

Tam, J.; Huissoon, J. Developing Psycho-Acoustic Experiments in Gas Metal Arc Welding International Conference on Mechatronics & Automation: Niagara Falls, CA, July 2005, pp.1112-1117.

Tam, J. Methods of Characterizing Gas-Metal Arc Welding Acoustics for Process Automation Master Dissertation in Mechanical Engineering, University of Waterloo, CA, 2005.

Venkatraman, B.; Menaka, M.;.Vasudevan M.; Baldev R. Thermography for Online Detection of Incomplete Penetration and Penetration Depth Estimation, In Proceedings of Asia-Pacific Conference on NDT, Auckland, New Zealand, November 5th–10th, 2006.

Walker, J. S.. Fourier Analysis and Wavelet Analysis, Proceeding of the AMS 1997, 44, No. 6, 658s-670s.

Wikle, H. III, R, Zee, B. Chin, "A Sensing System for Weld Process Control", Journal of Materials Processing Technology, no. 89-90, 1999, Pages 254-259.

Wikle III, H.C. Kottilingam. S.; Zee, R.H.; Chin, B.A. Infrared Sensing Techniques for Penetration Depth Control of the Submerged Arc Welding Process. J. Mater. Process. Technol. 2001, 113, 228–233.

Wu, C.S.; Gao, J.Q.; Hu, J.K. Real-Time Sensing and Monitoring in Robotic Gas Metal Arc Welding, Phys J. 2007, 18, 303s-310s.

Yaowen, W., Z. Pendsheng, "Plasma-arc welding Sound Signature for on-line Quality Control", Materials Science & Engineering Department, Taiyuan University of Technology, Taiyuan 030024, China, 2000, Pages 164-167.